Impact of granular filtration on ultrafiltration membrane performance as pre-treatment to seawater desalination in presence of algal blooms

Nour-Eddine Sabiri, Véronique Séchet, Pascal Jaouen, Maxime Pontié, Anthony Massé and Séverine Plantier

ABSTRACT

To mitigate fouling of the ultrafiltration (UF) membrane and improve permeate quality, we coupled granular filters (GF) with UF membrane as a pre-treatment for reconstituted seawater in the presence of algal bloom. Mono and bilayer granular filtrations were led at a mean velocity of 10 m h^{-1} over a 7-hour period. Both GF gave the same algal cell retention rate (∼63%) after 7 hours of filtration. Turbidity reduction rate was 50% for the monolayer filter and 75% for the bilayer filter. Resulting organic matter removal rate was 10% for the monolayer filter and 35% for the bilayer filter. Dissolved organic carbon removal was low (20%) with the bilayer filter and non-existent with the monolayer filter. GF-coupled UF reduced humic acids in the permeate (20%) compared with UF alone. Peak pressure of 3 bars was reached at the end of 30 minutes of UF in both direct UF or UF after monolayer GF. The filtrate from the bilayer GF enables UF over a longer period (7 hours).

Key words | algal bloom, fouling, granular filtration, pre-treatment, seawater, ultrafiltration

Nour-Eddine Sabiri (corresponding author)
Pascal Jaouen
Maxime Pontié
Anthony Massé
Séverine Plantier
Université de Nantes, GEPEA, UMR-CNRS 6144, 37
    Bd Université, BP 406,
44602 Saint-Nazaire Cédex,
France
E-mail: nour-eddine.sabiri@univ-nantes.fr

Véronique Séchet
Ifremer, Laboratoire Phycotoxines,
Centre de Nantes,
BP 21105,
44311 Nantes,
France

INTRODUCTION

Population growth is putting increased demand on water for farming, household use and industrial use, whereas freshwater supply is limited. Estimates for 2030 show that current freshwater resources (groundwater, surfacewater, etc.) cannot hope to meet demand. The effects are already being felt and will become even sharper in arid regions that are already water-stressed (Service 2006). Seawater desalination emerged decades ago as an alternative solution to the crisis of industry overdrawing freshwater resources. Desalination is increasingly being used around the world to provide people with needed freshwater, and already yields over 1% of global drinking water produced (Fievrez

et al. 2009). Two main desalination process technologies are currently in use: reverse osmosis (RO) and distillation, which drives 44% of global desalination capacity (Lauren et al. 2009). The choice between the two thermal processes (multi-flash or multi-effect) and RO essentially hinges on energy costs, quality of raw or desalinated water, and plant production capacity (Gaid & Treal 2007).

RO processes have several advantages over distillation processes. First, RO can treat higher-salinity water than distillation. Furthermore, the energy consumption of RO is low, often making RO-process seawater desalination plants more profitable than distillation-process plants at equally large production capacities. However, RO requires heavy pretreatment steps to obtain water that is clear enough to not cause excessive clogging of the membranes. All RO seawater desalination plants are exposed to low-to-moderate concentrations of algae, but many plants are located in algal bloom-

Uncorrected Proof

2   N.-E. Sabiri *et al.* | Seawater pre-treatment during a planktonic bloom before reverse osmosis step   Journal of Water Reuse and Desalination | in press | 2017

prone hotspots where concentrations can reach higher than 10^3 cells per mL (Edzwald & Haarhoff 2011). This makes pre-treatment prior to RO desalination a vital prerequisite (Voutchkov 2010a, 2010b).

A recent review by Jamaly *et al.* (2014) summarized the performance of RO coupled to various pre-treatment technologies. Conventional granular media filtration and membrane filtration are the main systems used before RO membranes in the field of desalination. Organic fouling remains a major challenge in the field of desalination-industry ultrafiltration (UF) pre-treatment systems (Resosudarmo *et al.* 2013). Various studies (Peter *et al.* 2005) have shown that a pre-treatment using the UF membrane systems for seawater desalination can significantly reduce the rate of membrane fouling and extend the life of RO membrane modules. Di Profio *et al.* (2011) studied the feasibility of using submerged hollow-fiber UF as seawater pre-treatment to engineer integrated membrane desalination systems under optimum conditions. Zhang *et al.* (2006) tested a UF system with and without coagulation of the raw water and confirmed that UF provided filtered water with high and constant quality, even with poor-quality raw seawater, which thus enhanced the reliability of the RO desalination plant. The flux of filtered seawater in a steady-state condition could be increased by the raw seawater coagulation. Abdessamad *et al.* (2008) showed that softening improves the limit permeate flux obtained with UF alone. Noelia *et al.* (2011) studied other RO pre-treatment alternatives in different configurations including coagulation, flocculation and maturation stages or just a coagulation stage followed by two pressurized multimedia filters. Recently, Andrea *et al.* (2014) compared slow sand filtration and microfiltration as pre-treatment for inland desalination via RO while Assiyeh *et al.* (2014) studied the effect of coagulation on fouling potential and removal of algal organic matter in seawater UF systems. Mitrouli *et al.* (2008) studied granular bed filtration of seawater using dual media by comparing Filtralite NC 1.5–2.5 mm on top of Filtralite HC 0.8–1.6 mm against anthracite coal on top of a sand layer to evaluate the performance on the basis of particulate removal from the feed water to obtain permeates of acceptable quality (in a first approach estimated by the silt density index, SDI) for feeding RO systems.

Any attempt to establish a fairly exhaustive analysis in this area would be difficult due to the many studies involved

and the various operating conditions employed. However, a common denominator through the literature is the aim to demonstrate how each configuration tested is geared to improve pre-treatment before the RO step. Our work builds on this effort. Here we studied granular media filtration coupled with UF to evaluate the impact on UF membrane clogging and permeate quality in the presence of artificial algal blooms. The originality of this work lies in different aspects: the seawater is reconstituted according to a reproducible protocol yielding an average composition that is representative of a natural seawater; the granular filtration tests are realized over long periods (approximately 7 hours) and entire filtrate is used to implement the coupling with the UF module; and all experiments are performed in similar operating conditions to industrial practice.

MATERIAL AND METHODS

Selection of model components and reconstituted seawater used for filtration tests

All seawater worldwide contains much the same families of components, but its component content varies according to tide, season, temperature, region, weather conditions, and so on. This variability means that experiments using natural seawater as a first resource for desalination process operations would be neither reproducible nor repeatable. Natural seawater contains mineral and natural organic matters in a dissolved state or in suspension. Table 1 compiles the main classes of compounds found in seawater and their

Table 1 | Average composition of real seawater (Copin-Montégut 1991; Gaid & Treal 2007; Leparc *et al.* 2007; Petry *et al.* 2007)

Classes of the compounds	Concentrations
Suspended matter	
Minerals	10 mg L^{-1}
Organics (phytoplankton)	10^3 cells L^{-1}
Dissolved matter	
Minerals (salts)	35 g L^{-1}
Organic matters	1 mgC L^{-1}
Humic substances (60%–80%)	0.6–0.8 mgC L^{-1}
Polysaccharides (20%–40%)	0.2–0.4 mgC L^{-1}

Uncorrected Proof

3   N.-E. Sabiri *et al.* | Seawater pre-treatment during a planktonic bloom before reverse osmosis step   Journal of Water Reuse and Desalination | in press | 2017

concentrations. In order to control and precisely know the characteristics of the feed suspension of the filtration processes, microalgae-free synthetic seawater was prepared at the laboratory to present very similar composition and concentration characteristics to real seawaters. Microalgae was subsequently added in order to simulate an algal bloom. Model compounds were selected to reconstitute the seawater and the concentrations were adjusted accordingly. Reconstituted seawater does not reflect the full complexity of real seawater but should make it possible to evaluate the contribution of the main components on fouling.

Seawater reconstitution needs to take into account mineral compound content and especially organic compound content which is the main driver of clogging problems in RO pre-treatment (Kennedy *et al.* 2008; Moonkhum *et al.* 2010).

Mineral matter – Particulate fraction

Research studying fouling in membrane processes often uses bentonite as it is already present in natural water (Naceur *et al.* 2003; Le-Clech *et al.* 2007; Mendret 2007; Pontié *et al.* 2012). Here we use bentonite to model the particulate mineral material of seawater. Particle size measured using a laser diffraction size analyzer ranged from 0 to 200 μm and content was 5 mg L^{-1}. The reconstituted seawater was also added with another mineral compound, kieselguhr or 'diatomite', again at 5 mg L^{-1}, to match the concentration found in Atlantic-type seawater (Prou 1993). The two compounds were held in an oven at 100 °C over one night before the preparation of the synthetic seawater.

Mineral matter – Dissolved fraction

A preparation of salts (INSTANT OCEAN™) was used to substitute the various salts present in seawater. This salts mixture is classically used in large-scale aquariums. This salt mixture was introduced at 35 g L^{-1} of RO water.

Organic matter – Dissolved fraction

The main organic matters in seawater are humic substances and polysaccharides, which are found in a colloidal particulate state and can contribute to the fouling of RO membrane

and pre-treatment processes in seawater desalination plants (Kinamura *et al.* 2004; Huang *et al.* 2007). Humic substances in natural seawater are often composed of 80% fulvic acids and 20% humic acids. Humic acids are widely used as models of humic substances (; Naceur *et al.* 2003; Katsoufidou *et al.* 2005; Costa *et al.* 2006). The humic acids used here were from Acros Organics (Humic acid sodium salt, (50–60% as humic acid), CA: 9005-32-7).

Studies on membrane clogging have often used alginates to model seawater polysaccharides (Katsoufidou *et al.* 2010; Sioutopoulos & Karabelas 2012). Alginates are salts of alginic acid which is a marine biopolymer obtained from brown macroalgae. Alginates were used here to model polysaccharides in synthetic seawater. They were obtained by dissolving alginic acid (Sigma-Aldrich) in a 35 g L^{-1} saltwater. Concentrations of humic acid and alginates were adjusted to 0.8 mgC L^{-1} and 0.2 mgC L^{-1}, respectively, in stock-solution synthetic seawater.
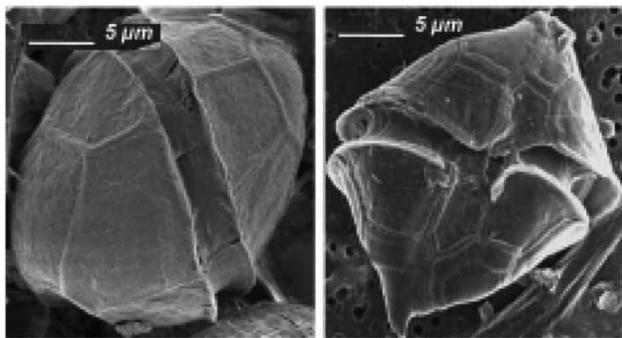
As humic acids and alginates interact in the presence of salts and form aggregates, stock solutions containing only the dissolved and colloidal fraction of humic acids and alginates were prepared by filtering raw humic and alginate suspensions through granular filters (GF)/F-grade Whatman filters (0.7 μm). Table 2 reports the average characteristics of the reconstituted seawater produced from 6 reconstitutions and a comparison with a range of values for natural seawater (6 different natural seawaters collected from different places around the world).

Selection of microalgae and simulation of the algal bloom

The pre-reconstituted seawater was doped with microalgae to simulate an algal bloom. For this, it was necessary to select and cultivate relevant micro-algae before adding it to the seawater. There are a number of species that can trigger algal blooms among which can be mentioned Alexandrim minutum (Bravo *et al.* (2008). This one is responsible for paralytic shellfish poisoning and it is one of the smallest toxic dinoflagellates observed during toxic blooms in French coastal waters. The dinoflagellate *Heterocapsa triquetra* (Figure 1) species was selected in this study for its morphological and size similarities with *A. minutum* and for its easy handling due to its harmless character.

Uncorrected Proof

4   N.-E. Sabiri et al. | Seawater pre-treatment during a planktonic bloom before reverse osmosis step   Journal of Water Reuse and Desalination | in press | 2017

Table 2 | Average characteristics of the reconstituted seawater and various natural seawaters (Copin-Montégut 1991; Gaid & Treal 2007; Leparc et al. 2007; Petry et al. 2007)

	Reconstituted seawater (average of 6 reconstitutions)	Natural seawater (average of different natural seawaters)
Turbidity (NTU)	3.49 ± 0.17	0.1–20
pH	7–8	7.4–8.5
MES (mg L^{-1})	8.69 ± 1.71	
SDI$_{15}$ (% min^{-1})	>6.6	>6.6
UV$_{254nm}$	$0.08 \pm 0,01$	0.6–18
TOC (mg L^{-1})	1.76 ± 0.97	0.8–4.0
DOC (mg L^{-1})	1.62 ± 0.81	
alginates (mgC L^{-1})	0.18 ± 0.11	
Humic acids (mgC L^{-1})	0.77 ± 0.07	
σ (20 °C) (mS cm^{-1})	41.84 ± 3.08	49–62
[Salts] (mg L^{-1})	$34,684 \pm 2.62$	
Na$^+$	$10,074 \pm 13$	10,945–15,000
K$^+$	332 ± 1	383–690
Mg^{2+}	$1,274 \pm 56$	1,334–1,660
Ca^{2+}	414 ± 6	405–780
Cl$^-$	$20,173 \pm 38$	19,080–26,500
Br$^-$	73 ± 1	45–67
NO^{3-}	158 ± 1	0.2–25
SO$_4^{2-}$	$2,185 \pm 15$	2,400–2,965

Figure 1 | Scanning electronmicrograph (SEM) of A. minutum (mean size: 20–23 μm) (left) and H. triquetra (mean size: 17–18 μm) (right). (A. minutum photo: GEPEA-UMR CNRS 6144; H. triquetra photo: CNRC-NRC).

Moreover, *Heterocapsa triquetra* also forms blooms that can appear at the same time as those of *Alexandrium minutum*, which means that their conditions of proliferation (and thus culture) are similar (Lassus et al. 2004; Labry et al. 2008).

Heterocapsa triquetra was cultured at the Phycotoxins laboratory of IFREMER–Nantes.

A sterilized 100 L reactor was inoculated from two 10 L balloons of microalgal culture. The culture medium consisted of 95% real seawater pre-filtered through a 0.2 μm cartridge filter and enriched with a type-L1 nutrient solution (Guillard & Hargraves 1993). The seawater simulating an algal bloom was prepared by adding a quantity of microalgae to obtain a concentration matching a bloom in the reconstituted seawater. According to the literature, *Alexandrium minutum* and *Heterocapsa triquetra* bloom at concentrations of about 10^5 and 10^3 cells mL^{-1}, respectively (Bravo et al. 2008). An average concentration of about 10^4 cells mL^{-1} was thus fixed for bloom reconstitutions in our experiments. To try to keep the same physiological state during our experiments, biomass used in preparing dilutions was obtained from continuous cultures, operating in the same conditions (pH, T, incident light and dilution rate). For each dilution, the algal culture had reached a steady state. At the moment when the biomass was collected, the mean daily growth rate was constant.

Porous media used in granular filtration

For the monolayer sand filter, the bed structure used for all tests consisted of a 75 cm deep layer of silica sand with an average grain diameter of 389 μm. For the bilayer filter, a 35 cm deep layer (upper section) of anthracite was mounted above a 75 cm deep sand layer. The anthracite size distribution ranged from 0.8 to 1.6 mm and apparent density was 680 kg m^{-3}. Image analysis (Sabiri et al. 2012) was used to measure various grain dimensions after first sifting the sand. Grading parameters are reported in Table 3 and Figure 2. The bilayer filter is characterized by a difference in density (1,385 kg m^{-3} for anthracite and 2,600 kg m^{-3} for sand) and a difference in effective size (0.8 to 1.6 mm for anthracite and 0.389 mm for sand). The porosity is determined by

Table 3 | Particle size characteristics of the sand used

d$_{mean}$ (μm)	d$_{min}$ (μm)	d$_{max}$ (μm)	d$_{10}$ (μm)	d$_{60}$ (μm)	d$_{50}$ (μm)	d$_{90}$ (μm)	Uniformity coefficient UC = d$_{60}$/d$_{10}$
389	38	589	306	413	407	481	1.35

Uncorrected Proof

5   N.-E. Sabiri *et al.* | Seawater pre-treatment during a planktonic bloom before reverse osmosis step   **Journal of Water Reuse and Desalination** | in press | 2017
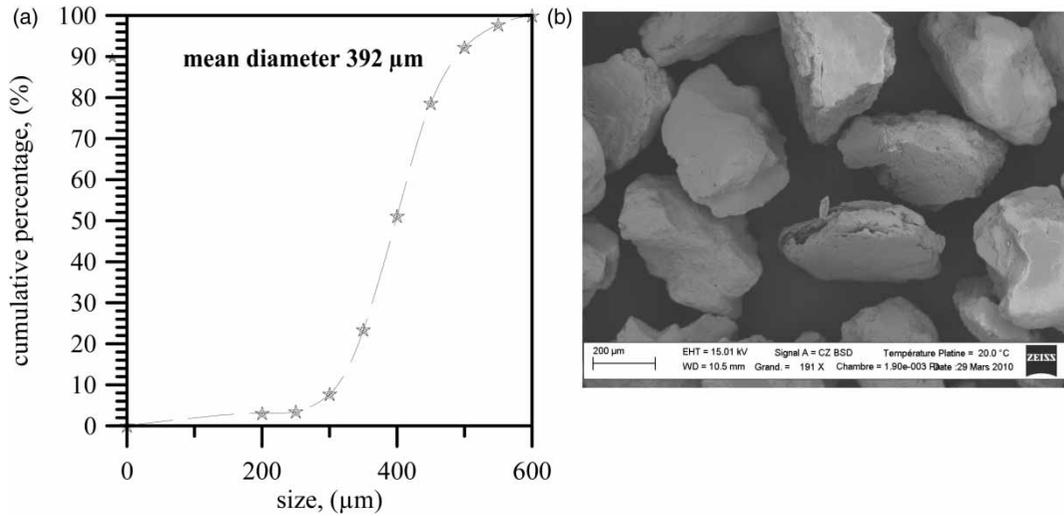

Figure 2 | (a) Representative cumulative particle size distribution of sand; (b) SEM image of the sand used.

subtracting the media volume from the total bed volume (water displacement technique). The porosity is equal to 0.43 for the sand section, and 0.56 for the anthracite section. The permeability, K, of the two layers of sand and anthracite was obtained using measurements of pressure gradient according to superficial velocity. The values obtained were approximately $9.51\ 10^{-1}$ (m^2) $\sim$95 Darcy for sand and $2.49\ 10^{-10}$ (m^2) $\sim$250 Darcy for anthracite. The disordered stacking of the sand or anthracite particles produces a complex geometry that is impossible to describe rigorously. However, an estimate of mean pore sizes with simplifying assumptions can be important information to describe the medium. Average diameter of the pores in each layer (anthracite or sand) is estimated from the following relationship:

$$d_{pore} = \sqrt{\frac{32K}{\varepsilon}} \tag{1}$$

where ε is estimated porosity. This relationship comes from the association of the Kozeny-Carman model with Poiseuille equation in a laminar flow in a tube. The average pore diameter values thus obtained were 84 μm for the sand and 125 μm for the anthracite.

Experimental setup used in granular filtration

The study was carried out using a lab-based pilot-scale granular filter. Figure 3 gives a schematic of the filtration system. The pilot consists of two plexiglass columns of 9 cm of internal diameter and 140 cm total height. Feed tank capacity is 240 L. A volumetric pump is used to ensure circulation through the system. A rotameter is placed at the inlet of each column to control the flow. The hydraulic system allows a dual operation: circulation into the bed in the descending direction during the filtration cycle; and circulation in the ascending direction during the post-filtration cleaning phase.

The feed flow rate in the filter is held constant throughout the filtration cycle (7 hours) and corresponds to a superficial velocity of 10 m/h. The tests were conducted at a temperature of 18–19 °C. Known quantities of each material (sand or anthracite) were introduced into the column. The system was backwashed for 5 min prior to each test in order to remove impurities. A period of clean-water filtration by fluidization process is performed after backwash to drive out any air bubbles in the packing, and allow the bed to settle down to good filtration performance. Stratification occurs after the fluidization step, and the finer and less dense grains are located at the upper layer like an industrial sand filter (Sabiri *et al.* 2012). The pressure gradient (ΔP) across the GF was measured during filtration using differential pressure sensors (DeltaBar, Endress + Hauser, Huningue, France).

Membrane UF process

The UF system (VMA industries, France) is presented in Figure 4. This unit is equipped with a module of
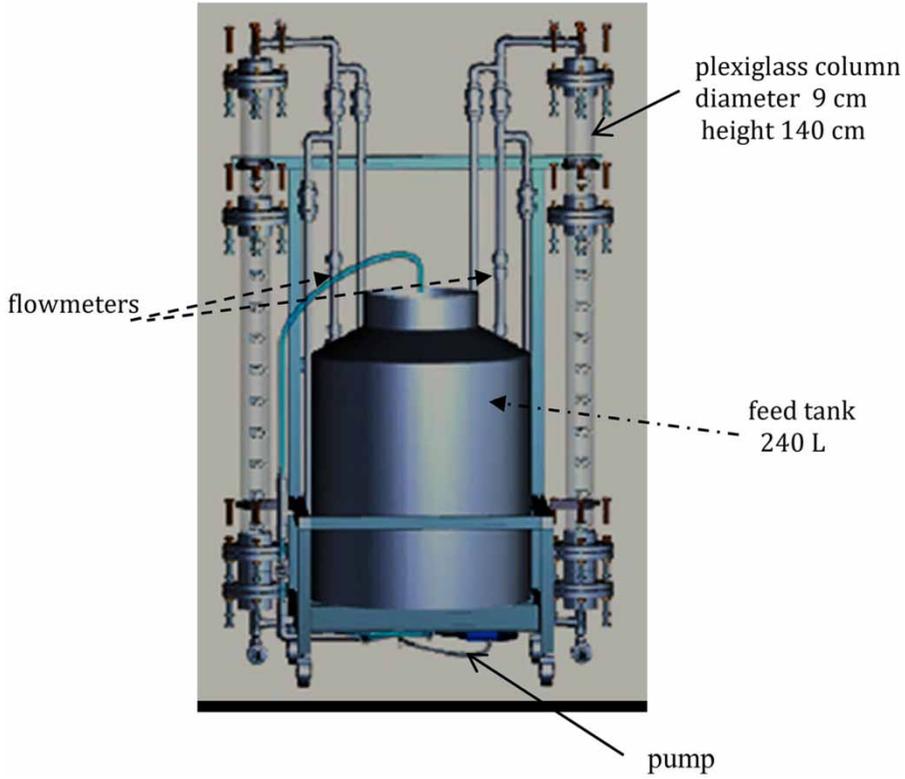
Uncorrected Proof

6   N.-E. Sabiri *et al*. │ Seawater pre-treatment during a planktonic bloom before reverse osmosis step   │ Journal of Water Reuse and Desalination │ in press │ 2017

Figure 3 │ Diagram of the granular filtration pilot.
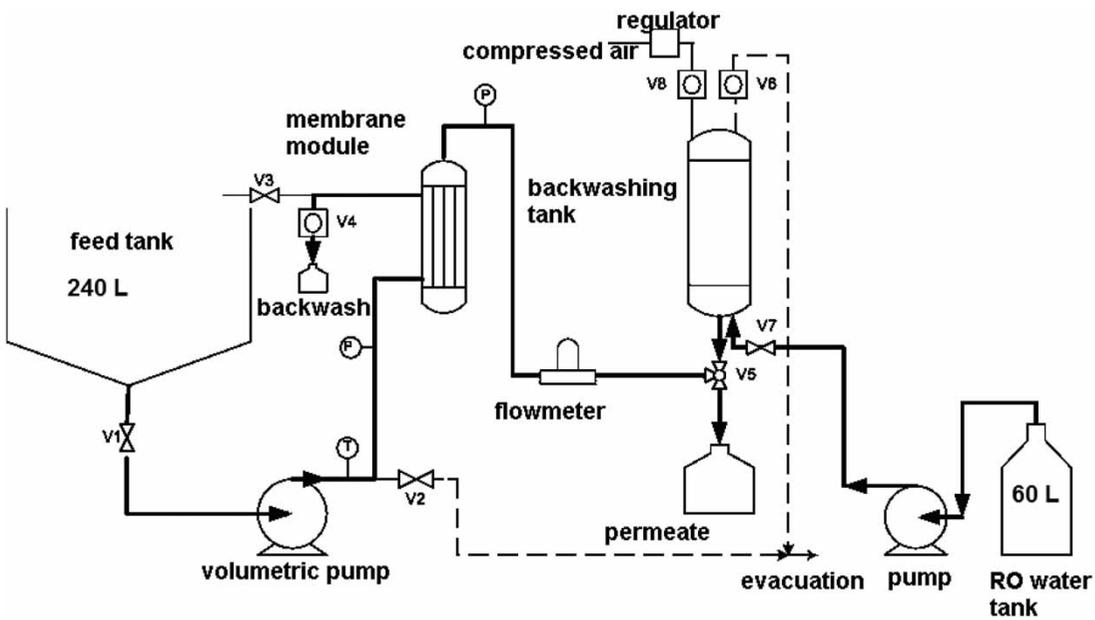
Figure 4 │ Schematic flow diagram of the membrane filtration pilot.

Uncorrected Proof

7   N.-E. Sabiri *et al.* | Seawater pre-treatment during a planktonic bloom before reverse osmosis step   Journal of Water Reuse and Desalination | in press | 2017

Polyvinylidene fluoride (PVDF) hollow fiber membranes (0.03 μm pore nominal diameter). Total membrane surface area is 0.28 m^2 and the external fiber diameter 1.8 mm. The module enables external/internal dead-end filtration through the fibers. The operating conditions used for UF were close to those used in real-world desalination plants. The permeate flux was fixed at a constant 100 L h^{-1} m^{-2} with a maximum pressure of 2.8 bars. Each UF sequence (cycle) consisted of a 30 min filtration followed by a 5 s relaxation period, a 15 s backwash, and a final 5 s relaxation period. Fouling resistances were determined using Darcy's law:

$$J = \frac{TMP}{(\mu R_t)} \tag{2}$$

where J is permeate flux (m^3 m^{-2} s^{-1}), TMP (Pa) is transmembrane pressure, μ is dynamic viscosity of permeate (Pa s), and R_t is total filtration resistance (m^{-1}). R_t is composed of three resistances in series:

$$R_t = R_m + R_{rf} + R_{irf} \tag{3}$$

where R_m, R_{rf} and R_{irf} refer to the hydraulic resistance of the membrane, reversible fouling resistance and irreversible fouling resistance, respectively. Reversible fouling resistance is defined as the fouling resistance removed after backwash and irreversible fouling resistance is defined as the fouling resistance remaining after backwash (Figure 5).

Analytical tools

Analyses were carried out on the feed and the filtrate at regular intervals (every 30 minutes) throughout filtration. The controlled parameters at the inlet and outlet of the process are the turbidity, granulometric distribution of algae
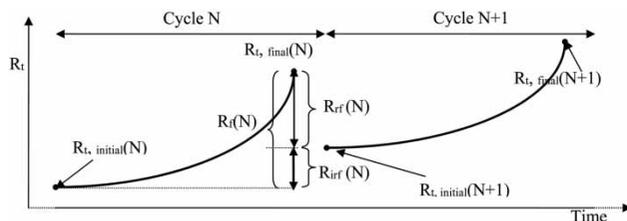
Figure 5 | Scheme of the various fouling resistances.

cells, concentration of the algae, total organic carbon (TOC), dissolved organic carbon (DOC), and specific UV absorbance at 254 nm.

The size distribution and concentration of the suspended algae is measured using a laser diffraction size analyzer (QICPIC, Sympatec, Clausthal-Zellerfeld, Germany) capable of analyzing particle sizes ranging from 1 micron to 2,000 microns. The bentonite used for reconstitution of seawater was also characterized using this technique. It consists of a LIXELL wet dispersion system through which the analyzed sample passes. Imaging was fixed at a frequency of 25 Hz during 240 seconds. Windox 5 software was then used to process the data in order to obtain the number of particles present in the sample stratified by size. Measurements were repeated 4 times for each sample and averaged to obtain a mean concentration. TOC and DOC were measured using the 680 °C combustion catalytic oxidation method with a Shimadzu TOC-L series analyzer after sample filtration at 0.7 μm. UV absorbance was measured at 254 nm on a UV/VIS spectrophotometer (Perkin Elmer). Turbidity was measured using a HACH 2,100AN Turbidimeter.

RESULTS AND DISCUSSION

Direct filtration on GF (monolayer and bilayer)

Comparison of the performances of the two GF

Reconstituted seawater was enriched with microalgae to obtain a concentration of 15,000 cells per mL. This suspension was used for filtration tests (mono or bilayer granular filtration and UF) alone or coupled.

At least three trials were performed with each of the sand filters (mono or bilayer). The efficiency of microalgae retention evolves in a similar way, with a fast drop at the beginning of filtration followed by a slower decrease (Figure 6). After 7 hours of filtration, the monolayer sand filter only retained 44% of microalgae while the bilayer filter retained over 52%. This shows that in terms of microalgae retention, the two filters demonstrate much the same performance level, as already observed by Henderson *et al.* (2008). As the error bars show (Figure 6), it is difficult to get perfectly repeatable filtrations results. Indeed, it is
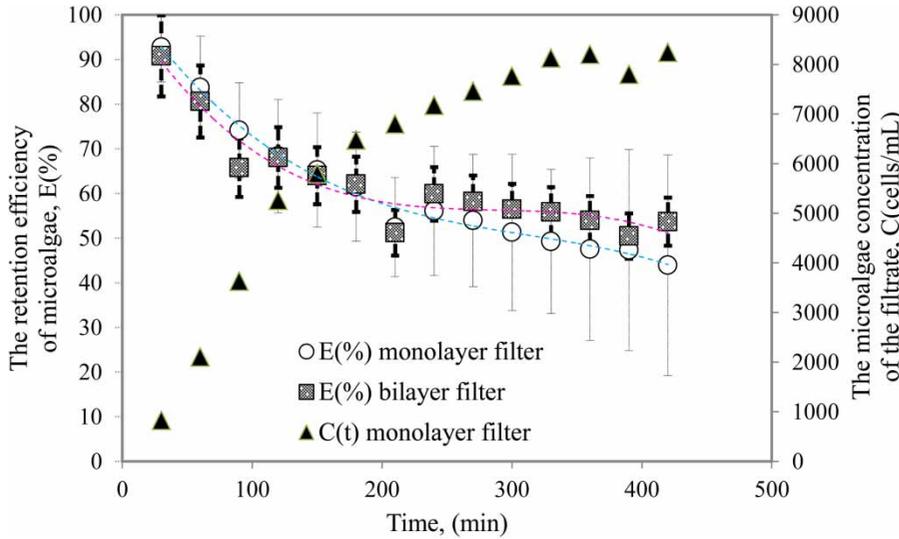
Uncorrected Proof

8   N.-E. Sabiri *et al.* | Seawater pre-treatment during a planktonic bloom before reverse osmosis step   Journal of Water Reuse and Desalination | in press | 2017

Figure 6 | Time–course plot of retention of algal cells by granular filtration.

already difficult to reconstitute identical algal blooms since there are living microorganisms that can vary in in physiological state from one experiment to another. In addition, the structural characteristics of the GF in each test are close but not identical. Pore size distribution can become slightly altered due to segregation at the first backwashing cycle. For these same reasons, real-world performance in seawater desalination plants can also be expected to change over time.

Mass balance analysis makes it possible to know the amount of accumulated microalgae inside the granular bed. Area between the curve and the *t*-axis can be used to calculate the quantity (number) N_{ac} of microalgae accumulated in the filter during filtration (Figure 6):

$$N_{ac} = C_0 Q \int_{t_0}^{t_1} \left(1 - \frac{C(t)}{C_0}\right) dt = C_0 Q \int_{t_0}^{t_1} E(t) dt \tag{4}$$

where C_0 is feed microalgae concentration, Q is feed flow rate, C(t) is filtrate concentration at time t, with t_0 and t_1 corresponding to the beginning and the end of the filtration cycle.

Figure 7 plots the variation of the ratio of the accumulated quantity N_{ac} of microalgae to total quantity brought to the filter ($N_0 = C_0 Q t$) over the course of the filtration cycle. Note that particle accumulation rate is slightly higher at the beginning of filtration and subsequently
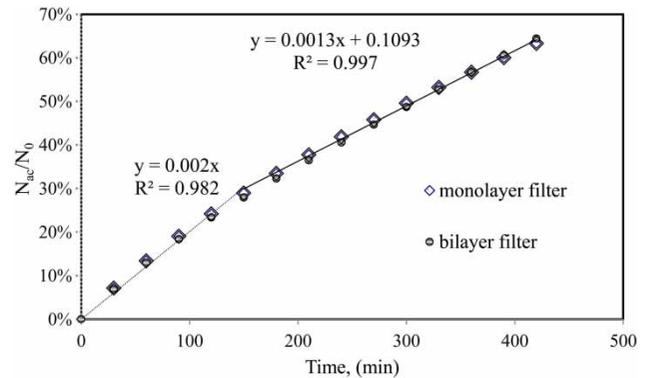

Figure 7 | Time–course plot of rate of algal particle accumulation during granular filtration with the two types of filters.

decreases. Particle accumulation rate was similar between the two filters, as total percentage of microalgae accumulated after 7 hours of filtration was approximately 63% for both types of filter. More than 30% of the microalgae are thus found in the filtrate.

Figures 8–10 report the results of the turbidity, TOC, DOC analyses, respectively. The turbidity and TOC profiles of the filtrate obtained from the monolayer or bilayer filter were similar. Indeed, turbidity and TOC increased rapidly at the beginning of filtration and had stabilized by the end. This stabilization occurs simultaneously with the stabilization of microalgae retention. DOC in the filtrate of the monolayer filter remained constant and close to feed DOC content whereas it appeared to decrease in the filtrate of
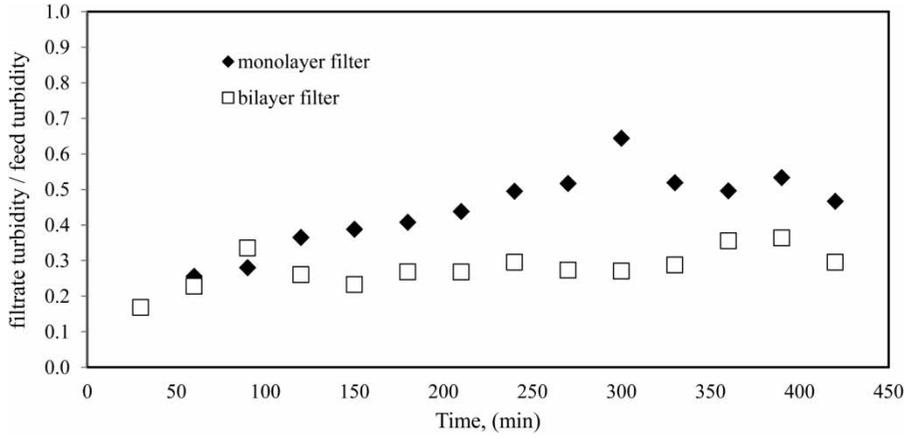
Uncorrected Proof

9   N.-E. Sabiri *et al.* │ Seawater pre-treatment during a planktonic bloom before reverse osmosis step   Journal of Water Reuse and Desalination │ in press │ 2017

Figure 8 │ Time–course plot of turbidity in the filtrate with the two types of filters.
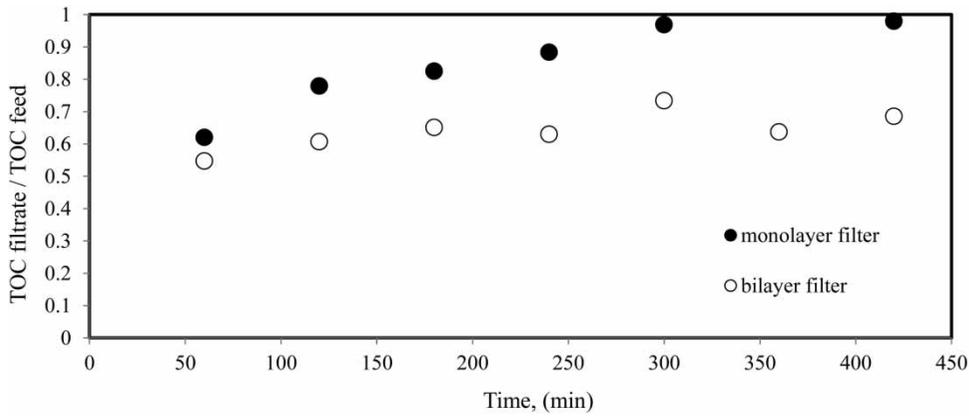

Figure 9 │ Time–course plot of TOC in the filtrate with the two types of filters.
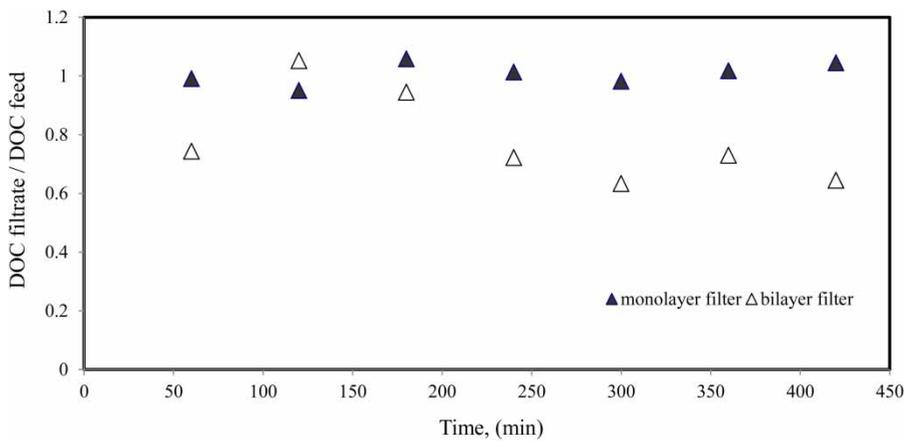

Figure 10 │ Time–course plot of DOC in the filtrate with the two types of filters.

Uncorrected Proof

10   N.-E. Sabiri *et al*. | Seawater pre-treatment during a planktonic bloom before reverse osmosis step   **Journal of Water Reuse and Desalination** | in press | 2017

the bilayer filter before stabilization. Anthracite could slightly reduce the DOC by adsorption. Overall, filtration with a bilayer filter gave better-quality water than filtration with a monolayer filter. The bilayer filter enabled a greater reduction of turbidity, TOC and DOC compared to the monolayer sand filter. Retention rate of humic substances (by 254-nm UV) was similar between the two filters and was only modest in both cases (26–28%).

Figure 11 reports the results of analysis on the size distribution of the particles present in the filtrate. The curves obtained had similar shapes for both types of filter and showed a peak between 15 and 20 microns corresponding to the average size of algal cells. Number of microalgae in the filtrate increased significantly during filtration and then tended to stabilize after 4 hours. The similarity of these distributions shows that all sizes are retained without much selectivity. However, cells larger than 15 μm are more easily retained.

Retention mechanisms for the monolayer filter

Previous work (Plantier 2013) suggests that 30 to 50% of particles are retained at the top of the filter. In the upper section of the filter, sand grains are finer and the ratio of sand grain diameter (d_g) to microalgae diameter (d_p) is less than 10 to promote the formation of a cake in the upper layers of filtrating bed. Indeed, according to McDowell-Boyer *et al*. (1986), if d_g/d_p ratio is <10, cake build-up overrides the trapping and adsorption mechanisms.

Indeed visual observation of the inlet bed confirmed the presence of a cake. Change of porosity in the cake can be determined by measuring the pressure drop on the total height of the bed and assuming that increases in pressure drop signal the presence of cake. The approach is based on considerations discussed below.

Assuming that microalgae are spherical with an average diameter d_p of 16 μm, then knowing the accumulated quantity N_{ac} of particles makes it possible to determine total volume $V_{\mu alg}$ occupied by the microalgae:

$$V_{\mu a\lg} = N_{ac}\left(\frac{4}{3}\pi\left(\frac{d_p}{2}\right)^3\right) \tag{5}$$

The interstitial volume can be calculated by the relationship: $V_{pores} = \varepsilon\,\Omega\,H$, where $\varepsilon \sim 0.43$ is the porosity estimated from the mass of sand and height of the filter bed (sand), Ω is filter cross-section (m^2) and H is height of bed (m)

The comparison between $V_{\mu alg}$ and V_{pores} shows that the microalgae retained during filtration occupy an extremely low volume (1%) of the total pore volume available. Consequently, pressure loss in the filter should not theoretically increase significantly during filtration. We can thus assume that the increase in pressure can be assigned mainly to the presence of the cake in the first layers.

In the case of cake filtration, total resistance R is the sum of two resistances in series, i.e. resistance of the filter medium R_f and resistance of the cake R_c. Then, if ΔP is total pressure drop, ΔP_c and ΔP_m are the pressure drop in
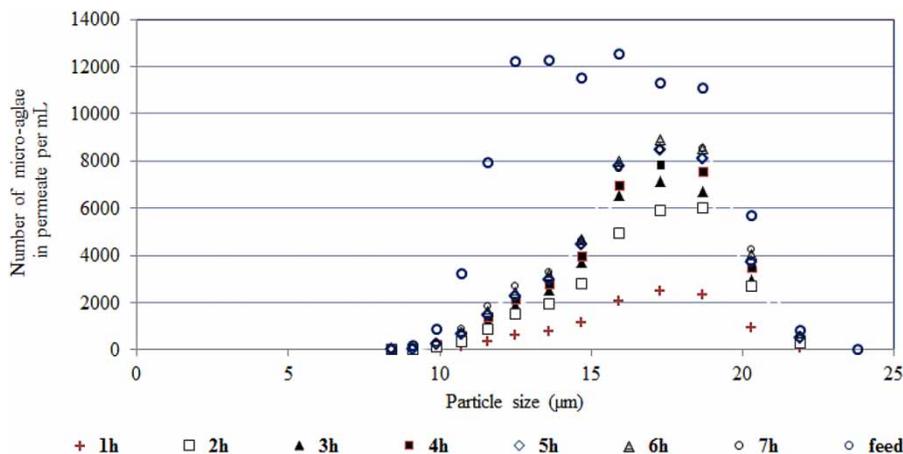
Figure 11 | Size distribution and concentration of micro-algae in the filtrate in granular filtration.

Uncorrected Proof

11   N.-E. Sabiri *et al.* | Seawater pre-treatment during a planktonic bloom before reverse osmosis step   Journal of Water Reuse and Desalination | in press | 2017

the cake and pressure drop in the porous medium (without cake), respectively. This gives:

$$\Delta P_c(t) = \Delta P(t) - \Delta P_m = \Delta P(t) - \Delta P(t=0) \tag{6}$$

As ΔP_m does not vary significantly during filtration, it can be assumed constant and equal to the initial value of the pressure drop through the filter. The granular filtration experiments were performed at a particles Reynolds number, $Re_p = (1/\mu)\rho d_p(Q/\Omega)$ of approximately 1.08. This value corresponds to the Darcy regime. The application of Darcy's law gives:

$$\Delta P_c = \mu \frac{L_c}{K_c}\left(\frac{Q}{\Omega}\right) = \mu R_c \left(\frac{Q}{\Omega}\right) \tag{7}$$

where μ is dynamic viscosity of the liquid, L_c is thickness of the cake, K_c is permeability of the cake, and R_c is resistance of the cake. The analogy between the Darcy's law and the Kozeny-Carman model for spherical particles gives:

$$R_c = 150 \frac{(1-\varepsilon_c)^2}{d_p^2 \varepsilon_c^3} L_c \tag{8}$$

If volume of microalgae accumulated in the cake is $V_{\mu c}$ and porosity in the cake is ε_c, then:

$$V_{\mu c} = (1-\varepsilon_c)\left(\frac{\pi D^2}{4}\right) L_c \tag{9}$$

Thus, relation (8) becomes:

$$R_c = 150 \frac{(1-\varepsilon_c)^2}{(d_p^2)\,\varepsilon_c^2} \frac{V_{\mu c}}{(1-\varepsilon_c)\left(\frac{\pi D^2}{4}\right)} \Rightarrow \frac{(1-\varepsilon_c)^3}{\varepsilon_c^2}$$

$$= \frac{R_c(d_p^2)}{150\,V_{\mu c}}\left(\frac{\pi D^2}{4}\right) \tag{10}$$

Relation (10) has the form of a third-degree equation: $\varepsilon_c^3 + p\varepsilon_c + q = 0$, where p and q are real values depending on R_c at each time t. Solving this equation affords the following real solution:

$$\varepsilon_c = \sqrt[3]{\frac{-q}{2} - \frac{1}{2}\sqrt{\frac{27q^2 + 4p^3}{27}}} + \sqrt[3]{\frac{-q}{2} + \frac{1}{2}\sqrt{\frac{27q^2 + 4p^3}{27}}} \tag{11}$$

One can then obtain the variation in cake porosity during filtration $\varepsilon_c(t)$ from the two functions R_c (t) and $V_{\mu c}$ (t). Based on previous results (Plantier 2013) for the retention profile, the accumulated volume of microalgae in the cake was estimated at approximately 30% of total volume retained along the filter during filtration. Function ε_c (t) is determined by this approach, and the results are shown in Figure 12(a).

The 'specific cake resistance' r (m^{-2}), defined as the ratio of resistance R_c to thickness, can also be estimated. Figure 12 reports the cake porosity and specific cake resistances calculated during filtration from the measured pressure drops. These r values range between 2.0×10^{13} and 8.8×10^{13} (m^{-2}). The filter cake is compressible, because its porosity decreases and its resistance increases with increasing pressure.

Retention mechanisms for the bilayer filter

Both filters have the same sand thickness. The bilayer filter has an additional layer of anthracite (35 cm), but otherwise all other operating conditions (flow rate and reconstituted bloom concentration) are the same. As shown in Figure 12(b), the increase in pressure drop measured across the global height of the bed (110 cm) during filtration using the bilayer filter did not exceed 10% of the value read at the beginning of filtration. There was no observable cake formation. This corroborates the previous assumption that the increase of pressure is attributed to cake build-up. The anthracite layer would therefore prevent cake formation and consequently reduce head loss. As the ratio of average anthracite diameter to average microalgae diameter is above 50, microalgae trapping in the pores of the anthracite layer is negligible, so the microalgae would be adsorbed (McDowell-Boyer *et al.* 1986; Benamar *et al.* 2007). Only this adsorption phenomenon plays a major role in microalgae retentionalgae. However, the bilayer sand filter retains as many microalgae as the monolayer filter (Figure 6). The absence of cake formation seems to be compensated by a greater adsorption capacity of anthracite compared to sand which would make it possible to retain as many microalgae as the cake when working with the monolayer filter.
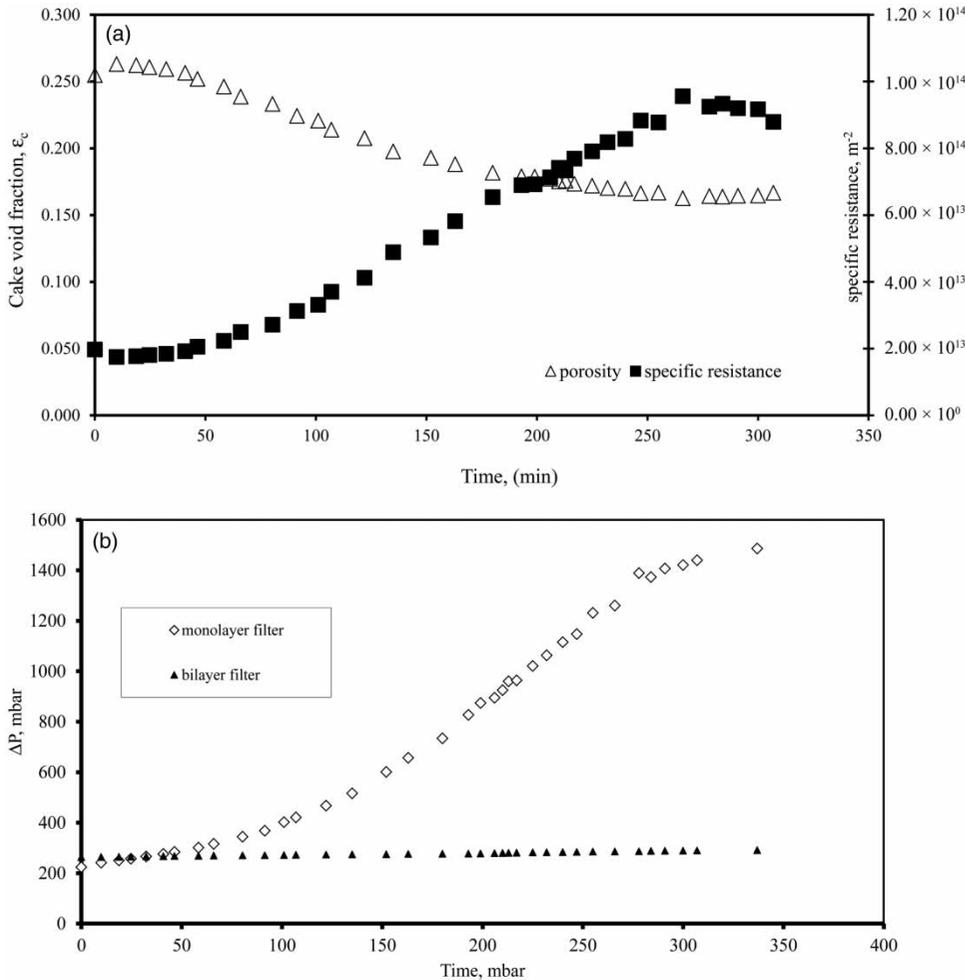
Uncorrected Proof

12   N.-E. Sabiri *et al.* │ Seawater pre-treatment during a planktonic bloom before reverse osmosis step   **Journal of Water Reuse and Desalination** │ in press │ 2017

Figure 12 │ (a) Void ratio and specific resistance of the cake in the monolayer filter; (b) Pressure drop obtained during the granular filtration (comparison between monolayer and bilayer filters).

Direct UF of reconstituted bloom

Filtration tests were also conducted by using UF without prior granular filtration. Algal suspensions (reconstituted seawater with microalgae) were used to directly feeding the UF system. These suspensions are identical to those used for the granular filtration. The reconstituted bloom clearly led to a rapid clogging of the membrane, and the filtration had to be stopped after 30 minutes because the maximum pressure (3 bars) recommended was reached. The SDI is determined at 2.1 bars according to ASTM D-4189-95 standard (ASTM 1995). It is defined as follows:

$$SDI_{(\%/\min)} = \frac{100(1 - t_0/t_f)}{t_T}$$

With t_0, the time required to filter the first 500 mL of the suspension (s), t_f, the time (s) required to obtain 500 mL of permeate after a period of time equal to t_T (min), usually 15 min. Millipore 0.45 μm nitrocellulose membrane (Ref. HAWP 04700) is used for SDI measurements. The values of SDI_{15} of permeates vary between 3.0 and 4.0% min^{-1}, and the turbidity is less than 0.2 NTU. The average values of different characteristics (TOC, UV_{254nm}, SDI_{15} and turbidity, algal cells) obtained in the UF permeate are shown in Table 4.

Interest of coupling a granular filter and an UF membrane

Implementing GF with an UF membrane as a single process before the RO step for seawater desalination does not seem

Uncorrected Proof

13   N.-E. Sabiri *et al.* | Seawater pre-treatment during a planktonic bloom before reverse osmosis step   Journal of Water Reuse and Desalination | in press | 2017

Table 4 | Average characteristics of waters produced (filtrate or permeate) by each process

	Monolayer filter	Monolayer filter + UF	Bilayer filter	Bilayer filter + UF	UF without GF
Turbidity (NTU)	4.09 ± 0.1	0.27 ± 0.10	2.02 ± 0.43	0.77 ± 0.30	0.12 ± 0.03
SDI_{15} (% min^{-1})	>6.6	4.8 ± 0.5	>6.6	3.2 ± 0.3	3.5 ± 0.3
UV_{254nm}	0.10 ± 0.01	0.06 ± 0.01	0.08 ± 0.01	0.06 ± 0.01	0.08 ± 0.01
TOC (mgC L^{-1})	7.74 ± 0.50	3.38 ± 0.12	3.06 ± 0.09	3.91 ± 1.43	3.10 ± 0.5
DOC (mgC L^{-1})	2.18 ± 0.02	–	2.84 ± 0.57	–	
H.triquetra (cells mL^{-1})	$8{,}430 \pm 17$	0	$7{,}351 \pm 49$	0	0

to be sufficient to maintain good productivity, especially in algal bloom periods. Indeed, the results obtained via this study show that the quality of the filtrates coming from mono or bilayer filters is not good enough for feeding RO membranes. We thus went on to investigate implementing a mono or bilayer filter upstream of the UF to evaluate the impact of this configuration on quality of the UF permeate and membrane fouling.

Quality of the waters produced

Overall filtrate of granular filtrations (~200 L) was collected, characterized and transferred to the feed tank of the UF module (Table 4). A dysfunction that took place after the 7th hour of filtration (i.e. at the end of filtration) on the monolayer filter meant that microalgae could have been released into the filtrate, which could partially explain the higher content of microalgae ($8{,}430 \pm 17$ cells mL^{-1} *vs* $7{,}351 \pm 49$ mgC L^{-1}) and TOC (7.74 ± 0.50 mgC L^{-1} *vs* 3.06 ± 0.09 mgC L^{-1}) in monolayer filtrate *versus* bilayer filtrate. DOC concentration was similar between the two filtrates (2.18 ± 0.02 mgC L^{-1} for the monolayer and 2.84 ± 0.57 mgC L^{-1} for the bilayer filter). The higher TOC value in monolayer filtrate would thus come from 0.7 μm-plus compounds, as DOC was measured after filtration on a 0.7 μm filter. The monolayer filtrate also had higher turbidity. The SDI_{15} and turbidity values obtained after passing through bilayer GF and were stable over filtration, at $3.2 \pm 0.3\%$ min^{-1} and 0.77 ± 0.30 NTU, respectively. The permeate produced by the coupling between the bilayer and the UF membrane could thus viably feed a spiral-wound membrane module, for which the recommended SDI_{15} and turbidity values are <3% min^{-1} and 0.5 NTU,

respectively. Average TOC concentration of the permeate obtained after coupling the bilayer filter and UF was 3.9 ± 1.4 mgC L^{-1}, which is higher than the value found at the UF inlet (3.06 ± 0.09 mgC L^{-1}) due to a outlier value for one of the permeate samples. Nevertheless, it appears that the amount of organic carbon which is retained by the UF membrane is rather small or negligible.

Membrane fouling

UF on the bilayer filter permeate continued for 14 cycles before reaching the maximum authorized pressure of membrane module, whereas UF on the monolayer filter permeate generated substantial membrane fouling and the maximum authorized pressure was reached after just 2 filtration cycles, i.e. in less than one hour of filtration (Figure 13(a)). Therefore, compounds such as microalgae and organic matter with a size higher than 0.7 μm could thus be the main drivers of monolayer filtrate fouling power. Fouling resistances were calculated over UF on the bilayer filter permeate. Average irreversible fouling resistance was low, at $1.7 \times 10^{11} \pm 1.2 \times 10^{11}$ m^{-1}, so most of the fouling is reversible and accounts for 79% of total fouling resistance on average (Figure 13(b)).

CONCLUSION

The results obtained here demonstrate similar performances of the two types of filters in terms of retention of algal cells. However, the bilayer filter works without forming a surface cake and thus leads to a lower pressure drop than with the monolayer filter. Furthermore, fluidization of the porous
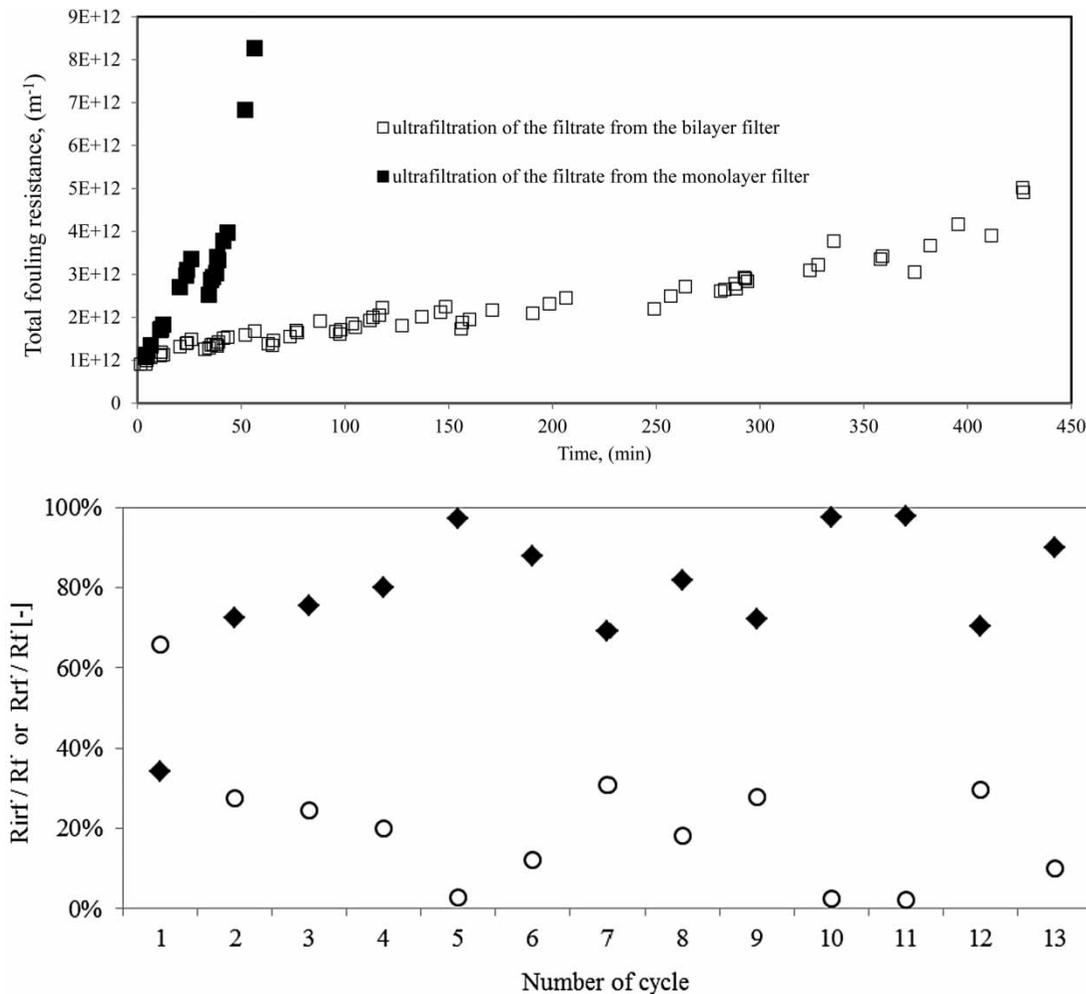
Uncorrected Proof

14   N.-E. Sabiri *et al.* │ Seawater pre-treatment during a planktonic bloom before reverse osmosis step   **Journal of Water Reuse and Desalination** │ in press │ 2017

Figure 13 │ (a) The total clogging resistance during UF after coupling with the monolayer or bilayer filter; (b) Changes of irreversible fouling resistance (R_{irf}) to total fouling resistance (R_f) ratio ($\bigcirc$) and reversible fouling resistance (R_{rf}) to total fouling resistance (R_f) ratio ($\blacklozenge$). (UF operated from bilayer filter output).

media during backwashing requires less energy and water when working with the bilayer filter. Coupling the two technologies (GF and UF) in series increases the retention of TOC and humic substances but without any significant impact on SDI_{15} or turbidity compared to a single UF system.

Both bilayer filter and monolayer filter gave similar-quality permeate, but the monolayer-filter permeate was unable to go through more than a couple of UF cycles. Indeed, pre-treatment with a bilayer sand filter delays membrane clogging, which effectively increases the duration of UF. Coupling the bilayer filter sand with UF might be an interesting pre-treatment system at the onset of an algal bloom. However, the coupling can be improved, particularly in terms of granular filtering by optimizing the height ratios of the two layers. On the other hand, replacing anthracite with more adsorbent materials to improve the retention of dissolved organic matter could also delay clogging at the UF stage.

REFERENCES

Abdessemed, D. & Nezzal, G. 2008 Coupling softening – ultrafiltration-like pre-treatment of sea water: case study of the Corso plant desalination (Algiers). *Desalination* **221**, 107–113.

ASTM 1995 *Standard Test Method for Silt Density Index (SDI) of Water*. ASTM International, West Conshohocken, PA, USA.

Uncorrected Proof

| 15 | N.-E. Sabiri *et al.* | Seawater pre-treatment during a planktonic bloom before reverse osmosis step | Journal of Water Reuse and Desalination | in press | 2017 |

Bravo, I., Vila, M., Maso, M., Figueroa, R. & Ramilo, I. 2008 *Alexandrium catenella* and *Alexandrium minutum* blooms in the Mediterranean Sea: toward the identification of ecological niches. *Harmful Algae* **7**, 515–522.

Carman, P. C. 1937 Fluid flow through granular beds. *Transactions of the Institution of Chemical Engineers* **15**, 150–166.

Copin-Montégut, G. 1991 Chimie de l'eau de mer, Institut Océanographique, p. 320 (in French).

Corral, A. F., Yenal, U., Strickle, R., Yan, D., Holler, E., Hill, C., Ela, W. P. & Arnold, R. G. 2014 Comparison of slow sand filtration and microfiltration as pre-treatments for inland desalination via reverse osmosis. *Desalination* **334**, 1–9.

Costa, A., De Pinho, M. & Elimelech, M. 2006 Mechanisms of colloidal natural organic matter fouling in ultrafiltration. *Journal of Membrane Science* **281**, 716–725.

Di Profio, G., Xiaoshen, J., Curcio, E. & Drioli, E. 2011 Submerged hollow fiber ultrafiltration as seawater pre-treatment in the logic of integrated membrane desalination systems. *Desalination* **269**, 128–135.

Edzwald, J. K. & Haarhoff, J. 2011 Seawater pre-treatment for reverse osmosis: chemistry, contaminants, and coagulation. *Water Research* **45**, 5428–5440.

Gaid, K. & Treal, Y. 2007 Le dessalement des eaux par osmose inverse: l'expérience de Véolia Water. *Desalination* **203**, 1–14.

Greenlee, L. F., Lawler, D. F., Freeman, B. D., Marrot, B. & Moulin, P. 2009 Reverse osmosis desalination: water sources, technology, and today's challenges. *Water Research* **43**, 2317–2348.

Guillard, R. & Hargraves, P. 1993 Stichochrysis immobilis is a diatom, not a chrysophyte. *Phycologia* **32**, 234–236.

Huang, H., Lee, N., Yong, T., Amy, G., Lozier, J. & Jacangelo, J. 2007 Natural organic matter fouling of low-pressure, hollow fiber membranes: effects of NOM source and hydrodynamic conditions. *Water Research* **41**, 3823–3832.

Jamaly, S., Darwish, N. N., Ahmed, I. & Hasan, S. W. 2014 A short review on reverse osmosis pre-treatment technologies. *Desalination* **354**, 30–38.

Katsoufidou, K., Yiantsios, S. & Karabelas, A. 2005 An experimental study of UF membrane fouling by humic acids and sodium alginate solutions: the effect of backwashing on flux recovery. *Desalination* **220**, 214–227.

Katsoufidou, K., Sioutopoulos, D., Yiantsios, S. & Karabelas, A. 2010 UF membranes fouling by mixtures of humic acids and sodium alginate: fouling mechanism and reversibility. *Desalination* **264**, 220–227.

Kennedy, M., Kamanyi, J., Heijman, B. & Amy, G. 2008 Colloidal organic matter fouling of UF membranes: role of NOM composition & size. *Desalination* **220**, 200–213.

Kinamura, K., Hane, Y., Watanabe, Y., Amy, G. & Ohkuma, N. 2004 Irreversible membrane fouling during ultrafiltration of surface water. *Water Research* **38**, 3431–3441.

Labry, C., Erard-Le Denn, E., Chapelle, A., Fauchot, J., Youenou, A., Crassous, M., Le grand, J. & Lorgeoux, B. 2008 Competition for phosphorus between two dinoflagellates: a toxic Alexandrium minutum and a non-toxic Heterocapsa triquetra. *Journal of Experimental Marine Biology and Ecology* **358**, 124–135.

Lassus, P., Baron, R., Garen, P., Truquet, P., Masselin, P., Bardouil, M., Leguay, D. & Amzil, Z. 2004 Paralytic shellfish poison outbreaks in the Penze estuary: environmental factors affecting toxin uptake in the oyster, Crassostrea gigas. *Aquat. Living Resour.* **17**, 207–214.

Le-Clech, P., Marselina, Y., Ye, Y., Stuetz, R. & Chen, V. 2007 Visualisation of polysaccharide fouling on microporous membrane using different characterisation techniques. *Journal of Membrane Science* **290**, 36–45.

Leparc, J., Rapenne, S., Courties, C., Lebaron, P., Croué, J.-P., Jacquemet, V. & Turner, G. 2007 Water quality and performance evaluation at seawater reverse osmosis plants through the use of advanced analytical tools. *Desalination* **203**, 243–255.

Mendret, J. 2007 *Mise au point de méthodes de caractérisation du colmatage de membranes: application à la caractérisation in situ d'un depot particulaire en ultrafiltration frontale en lien avec les performances du procédé. Thesis*, Institut Nationale des Sciences Appliquées, Toulouse, p. 246 (in French).

Mitrouli, S. T., Yiantsios, S. G., Karabelas, A. J., Mitrakas, M., FØllesdal, M. & Kjolseth, P. A. 2008 Pre-treatment for desalination of seawater from an open intake by dual-media filtration: pilot testing and comparison of two different media. *Desalination* **222**, 24–37.

Moonkhum, M., Lee, Y. & Seok, Y. 2010 Review of seawater natural organic matter fouling and reverse osmosis transport modeling for seawater reverse osmosis desalination. *Desalination and Water Treatment* **15**, 92–107.

Naceur, M., Ait Messaoudene, N. & Aggoun, A. 2003 Microfiltration reinforced adsorption of humic acids onto modified Algerian clay. *Desalination* **158**, 1–3.

Petry, M., Sanz, M., Langlais, C., Bonnélye, V., Durand, J. U.-P., Guevara, D., Mantovani Nardes, W. & Homma Saemi, C. 2007 The El Coloso (Chile) reverse osmosis plant. *Desalination* **203**, 141–152.

Plantier, S. 2013 'Procédés de traitement d'eau de mer avant osmose inverse en présence d'efflorescences algales'. *PhD thesis*, GEPEA UMR-CNRS 6144, CRTT, 37 Bd de l'université, 44602 Saint-Nazaire Cedex (France). (In French).

Plantier, S., Castaing, J. B., Sabiri, N. E., Massé, A., Jaouen, P. & Pontié, M. 2012 Performance of a sand filter in removal of algal bloom for SWRO pre-treatment. *Desalination and Water Treatment* **51**, 1838–1846.

Pontié, M., Thekkedath, A., Kecili, K., Dach, H., De Nardi, F. & Castaing, J. B. 2012 Clay filter-aid in ultrafiltration (UF) of humic acid solution. *Desalination* **292**, 73–86.

Prou, S. 1993 *Etude du pouvoir colmatant des contaminantes non-dissous de l'eau de mer.* Rapport de fin d'étude approfondies, Univsersité de Nantes, Saint-Nazaire, 48p. (In French).

Quevedo, N., Sanz, J., Ocen, C., Lobo, A., Temprano, J. & Tejero, I. 2011 Reverse osmosis pre-treatment alternatives:

Uncorrected Proof

16   N.-E. Sabiri et al. │ Seawater pre-treatment during a planktonic bloom before reverse osmosis step   **Journal of Water Reuse and Desalination** │ in press │ 2017

demonstration plant in the seawater desalination plant in Carboneras, Spain. *Desalination* **265**, 229–236.

Resosudarmo, A., Ye, Y., Le-Clech, P. & Chen, V. 2013 Analysis of UF membrane fouling mechanisms caused by organic interactions in seawater. *Water Research* **47**, 911–921.

Sabiri, N. E., Castaing, J. B., Massé, A. & Jaouen, P. 2012 Performance of a sand filter in removal of micro-algae from sea water in aquaculture production systems. *Environmental Technology* **33**, 667–676.

Service, R. F. 2006 Desalination freshens up. *Science* **313**, 1088–1090.

Sioutopoulos, D. & Karabelas, A. 2012 Correlation of organic fouling resistances in RO and UF membrane filtration under constant flux and constant pressure. *Journal of Membrane Science* **407–408**, 34–46.

Tabatabai, S. A. A., Schippers, J. C. & Kennedy, M. D. 2014 Effect of coagulation on fouling potential and removal of algal organic matter in ultrafiltration pre-treatment to seawater reverse osmosis. *Water Research* **59**, 283–294.

Voutchkov, N. 2010a *Seawater Pre-Treatment*. Water Treatment Academy, Bangkok, Thailand.

Voutchkov, N. 2010b Considerations for selection of seawater filtration pre-treatment system. *Desalination* **261**, 354–364.

Wolf, O. H., Siverns, S. & Monti, S. 2005 UF membranes for RO desalination pre-treatment. *Desalination* **182**, 293–300.

Zhang, J. D., Liu, Y. W., Gao, S. M., Li, C. Z., Zhang, F., Zen, H. M. & Ye, C. S. 2006 Pilot testing of outside-in UF pre-treatment prior to RO for high turbidity seawater desalination. *Desalination* **189**, 269–277.